Received: 6 February 2024 | Revised: 29 April 2024 | Accepted: 30 May 2024

DOI: 10.1111/mec.17462

ORIGINAL ARTICLE

MOLECULAR ECOLOGY WILEY

Isolation by environment and its consequences for range shifts with global change: Landscape genomics of the invasive plant common tansy

Ryan Briscoe Runquist | David A. Moeller

Department of Plant and Microbial Biology, University of Minnesota, St. Paul, Minnesota, USA

Correspondence
Ryan Briscoe Runquist, Department of Plant and Microbial Biology, University of Minnesota, 140 Gortner Laboratory, 1479 Gortner Ave, St. Paul, MN 55108, USA.
Email: rbriscoe@umn.edu

Funding information
Minnesota Invasive Terrestrial Plants and Pests Center through the Environment and Natural Resources Trust Fund

Handling Editor: Ana Caicedo

Abstract

Invasive species are a growing global economic and ecological problem. However, it is not well understood how environmental factors mediate invasive range expansion. In this study, we investigated the recent and rapid range expansion of common tansy across environmental gradients in Minnesota, USA. We densely sampled individuals across the expanding range and performed reduced representation sequencing to generate a dataset of 3071 polymorphic loci for 176 individuals. We used non-spatial and spatially explicit analyses to determine the relative influences of geographic distance and environmental variation on patterns of genomic variation. We found no evidence for isolation by distance but strong evidence for isolation by environment, indicating that environmental factors may have modulated patterns of range expansion. Land use classification and soils were particularly important variables related to population structure although they operated on different spatial scales; land use classification was related to broad-scale patterns and soils were related to fine-scale patterns. All analyses indicated a distinctive genetic cluster in the most recently invaded portion of the range. Individuals from the far northwestern range margin were separated from the remainder of the range by reduced migration, which was associated with environmental resistance. This portion of the range was invaded primarily in the last 15 years. Ecological niche models also indicated that this cluster was associated with the expansion of the niche. While invasion is often assumed to be primarily influenced by dispersal limitation, our results suggest that ongoing invasion and range shifts with climate change may be strongly affected by environmental heterogeneity.

KEYWORDS
climate change, ecological niche models, gene flow, leading range edge, local adaptation, population genetic structure

1 | INTRODUCTION

Range expansion of invasive species represents a major aspect of global change facing ecosystems. Invasive species movement across landscapes is modulated by a variety of genetic and ecological factors (Dlugosch et al., 2015; Lee, 2002). Losses of genetic variation may occur during rapid range expansion due to successive genetic bottlenecks (Dlugosch & Parker, 2008; Nei et al., 1975; but see Lake et al., 2023; Roman & Darling, 2007). Losses of variation may stymie invasion because of inbreeding depression or a limited capacity to adapt to novel environments (Frankham, 2005; but see Dlugosch et al., 2015; Oduor et al., 2016). However, some studies show that invasive species retain genetic variation for ecologically important traits and adaptive capacity despite losses of DNA sequence variation (Dlugosch & Parker, 2008; Hodgins et al., 2018; Lake et al., 2023). Over shorter timescales, the pattern and extent of range expansion may be determined by the distribution of suitable habitat. Comparatively little is understood about how environmental heterogeneity influences pathways of movement, particularly during rapid invasions. Recent developments in landscape genomics provide an opportunity to test whether (and to identify which) environmental factors have facilitated or inhibited invasion (Barrett, 2015; Clements & Ditommaso, 2011; Clements & Jones, 2021; Tomiolo & Ward, 2018).

Invasion history may influence the geography of genetic variation in several ways. The number and geographic origin of colonists influence genetic variation in founding populations (Baker & Stebbins, 1965; Dlugosch & Parker, 2008). Following introduction, the nature of population dynamics can be particularly important for the amount of genetic variation at leading range edges. Successive founder events during range expansion typically result in losses of heterozygosity and rare alleles because genetic drift is stronger at greater distances from the location of introduction (Baker & Stebbins, 1965; Nei et al., 1975; Peter & Slatkin, 2013; Slatkin & Excoffier, 2012). Rapid range expansion may also cause allele surfing, where new mutations arising at the invasion front rapidly increase in frequency regardless of their selection coefficient (Hallatschek et al., 2007; Klopfstein et al., 2006; Peter & Slatkin, 2013; Slatkin & Excoffier, 2012). In these cases, range expansion tends to affect levels of diversity and the geographic structure of variation. By contrast, when range expansion involves high rates of long-distance dispersal (as opposed to wave-like expansion), there are unlikely to be clear patterns of population structure (Ibrahim et al., 1996).

Over long time periods, the signature of invasion history on population genomic structure should erode due to ongoing migration, drift, and adaptation. At migration–drift equilibrium, we expect to find isolation by distance (IBD), whereby there is a positive correlation between genetic and geographic distance (Cox & Durrett, 2002; Kimura, 1964; Kimura & Weiss, 1964; Wright, 1943). In invasive species, IBD is not necessarily expected or observed (Hutchison & Templeton, 1999; Slatkin, 1993). The absence of IBD may occur because of rapid range expansion and stochastic long-distance dispersal events, which are common during invasion (Hutchison & Templeton, 1999; Slatkin, 1987, 1993; Wright, 1943). Conversely, IBD may be observed if the invasion occurred long enough in the past that there is migration–drift equilibrium. A signature of IBD may be observed if an invasion is the result of multiple introductions into different geographic regions that have not had sufficient time for expansion and admixture (Bradburd et al., 2013; Sexton et al., 2014; Taylor & Keller, 2007; van Strien et al., 2015). Finally, deviations from IBD may suggest that environmental factors have caused particular geographic pathways for movement such that distance is not a strong predictor of genetic distance.

Populations from analogous environments may exhibit greater genetic similarity than those from geographically close locations (i.e. isolation by environment [IBE]; Bradburd et al., 2013; Sexton et al., 2014; Shafer & Wolf, 2013; Wang & Bradburd, 2014; Wang et al., 2013). Whereas IBD may be unlikely during rapid invasion, IBE could arise if invasion pathways are modulated by particular environments. Adaptive differentiation can lead to patterns of IBE when there is strong selection against migrants from different environments (Räsänen & Hendry, 2008). For invasive species, adaptation may increase the set of environments available for invasion or allow for rapid responses to future climate change (DeMarche et al., 2019; Gallien et al., 2012). Indeed, local adaptation has been detected as often in non-native as native species (Oduor et al., 2016). However, patterns of IBE are also possible due to non-adaptive processes that decouple geographic distance and genetic similarity, such as variation in migration across environmental gradients (e.g. different vegetation types) or geographic features that function as barriers to migration (e.g. rivers, mountains or cropland; Bradburd et al., 2018; Marcus et al., 2021; Petkova et al., 2016; Sexton et al., 2014; Shafer & Wolf, 2013; Yang et al., 2020). In an applied context, determining environmental drivers of movement can help prioritize eradication efforts and identify habitats at risk of future invasion (Peterman & Pope, 2021).

Adaptation to new environments during invasion may change the nature or breadth of the ecological niche. Land managers often use ecological niche models (ENMs) to develop invasion forecasts and management planning (Guisan et al., 2014; Peterson & Vieglais, 2001). These models rely on accurate characterizations of a species ecological niche, however, the models generally do not account for adaptation or dispersal limitation (Atwater & Barney, 2021; Veloz et al., 2012; Yates et al., 2018). Increases in overall niche breadth via adaptation may allow for colonization of new habitats and increase the potential range size of the invader (Kawecki, 2008; Putra et al., 2023; Tomiolo & Ward, 2018). Additionally, adaptive divergence may lead to the development of distinctive genotypes that occupy only a subset of the species-level niche. For example, Johnsongrass exhibits adaptive differentiation in niche between agricultural and non-agricultural populations, which has broadened the overall species niche and increased the potential for economic damage (Atwater et al., 2016; Lakoba et al., 2021). Niche shifts such as this may enable greater invasive spread into regions previously deemed

low risk. Overall, understanding niche evolution may be important for predicting range expansion and developing habitat-specific management strategies (Kawecki, 2008; Mouquet et al., 2015).

In this study, we investigated landscape genetic variation of the invasive species, common tansy (*Tanacetum vulgare*), to determine how environmental factors shaped dispersal pathways during invasion. We also tested whether areas of recent invasion involved niche expansion. Common tansy is an economically damaging invasive species in North America that degrades rangelands, impedes restoration efforts and outcompetes native plants. It is especially problematic across the northern tier of the United States and is particularly abundant in Minnesota, where invasive spread has been recent and rapid (Figure 1; LeCain & Sheley, 2014; MN Department of Agriculture: Common tansy, 2023; MN Department of Natural Resources: Common Tansy, 2023; White, 2001). First, we densely sampled individuals across the invaded range in Minnesota to test for fine-scale genetic structure. We assessed whether landscape genetic structure was best explained by geographic distance (IBD) in both spatial and non-spatial frameworks. We then developed environmentally informed genetic resistance models to test which environmental factors influenced pathways of movement (IBE). Last, we constructed ENMs of individual genetic clusters to test whether recovered landscape genetic structure also represented differences in the ecological niche. Together, our analyses provide insight about the factors that have shaped recent range expansion and may impede continued invasion.

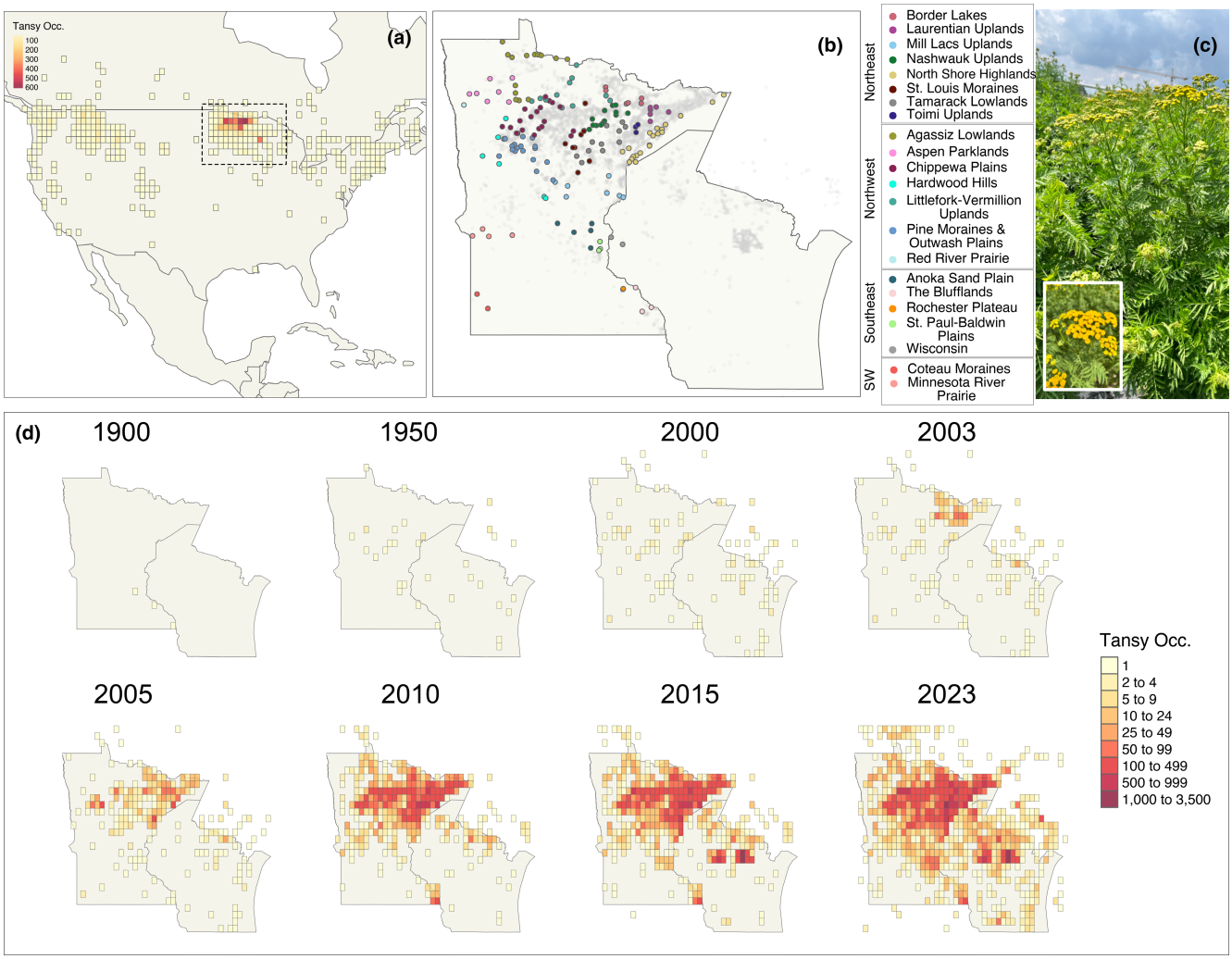

FIGURE 1 (a) Distribution of common tansy in North America based on occurrence records from EDDMaps and GBIF. Grid cells with darker red coloration have more occurrences, whereas grid cells with yellow coloration have very few occurrences. The dashed box outline indicates the study region centred on Minnesota. (b) Distribution of common tansy in Minnesota and Wisconsin. Sampled populations are coloured by MN ecological subsection. The subsections are divided roughly into four geographic quadrants: northwest, northeast, southwest and southeast. The remaining occurrence records from EDDMaps and GBIF are shown as light grey dots. (c) Photograph of flowering common tansy plant with an inset of a cluster of inflorescences. (d) Timeline of common tansy records in Minnesota and Wisconsin (See Supplementary Materials for more detailed methods). Grid cell coloration indicates the cumulative number of records up through the year indicated. Yellow indicates very few records (<10); grid cells with red colours indicate 100's–1000's of records.

2 | MATERIALS AND METHODS

2.1 | Natural history

Common tansy (*Tanacetum vulgare* L.; Asteraceae) is an herbaceous, C3 perennial native to Europe (Figure S1). Individuals form large multi-stemmed plants with shallow root systems (Jacobs, 2008). Flowers are largely self-sterile, although mixed-mating has been documented; outcrossing may occur via a diverse array of insects (Figure 1c; Jacobs, 2008; LeCain & Sheley, 2014). Recruitment occurs via seeds, rhizomes and root fragments. Seeds lack special adaptations for dispersal but are likely moved by wind, water and human activity (White, 1997).

Common tansy is distributed across the northern tier of the United States and southern tier of Canada with very few occurrences south of 40° S latitude (Figure 1a). It was introduced to the northeastern United States from Eurasia as early as the 1600s (Clasen et al., 2011; Lake et al., 2020; Mack, 2003; Mitich, 1992; USDA Plants Database, 2023). Minnesota has the highest density of reported occurrences in the United States (Figure 1a) with the earliest record from 1878 in the southeastern corner of the state (Mack, 2003; Roberts, 1878). During the 20th century, infrequent occurrences were recorded, primarily in the northeastern and central areas of the state (Figure 1d). In the past 20 years, the distribution rapidly expanded, first into northeastern MN, followed by expansion west and south, and last into northwestern MN. In Minnesota, the southern and western range margins occur along an ecological transition from cooler, wetter forests, to warmer, drier prairie grasslands. Occurrence records from the northwest are all recent (nearly all <10 years old) and are much less frequent than other areas (Figure 1d). Within its range, common tansy typically occurs in open habitats and is a weed of pastures and rangelands. Plants are avoided by livestock and insect herbivores because they produce a diverse set of terpenes that are toxic (Wolf et al., 2012).

Common tansy is diploid with c. 4300 Mbp per haploid genome (Keskitalo et al., 1998). Genomic resources have not been developed for the genus *Tanacetum*; past studies have involved a handful of populations and few molecular markers (e.g. microsatellites; Clasen et al., 2011).

2.2 | Sample collections

In summer/fall 2019, we collected individuals from 176 localities in the invaded range of Minnesota ($n = 174$) and western Wisconsin ($n = 2$), USA. These populations spanned the entire distribution of common tansy in Minnesota and represented the most fine-scale environmental variation (Figure 1b). Populations occur in 22 of the 26 ecological subregions (MN Department of Natural Resources Ecological Classification System, 2023; Figure S2), which describe areas with similar ecological features such as climate, topography and soils. Throughout the paper, we will refer to populations by ecological subregion (Table S1; Figures 1b and S3).

We collected leaves from one individual per population, dried leaf tissue in silica gel and extracted DNA using Genesee Zymo Quick-DNA Plant/Seed Miniprep Kits. Reduced representation sequencing was performed with Illumina NextSeq at the U. of Minnesota Genomics Center. Briefly, dual-indexed GBS libraries were created with the enzyme combination BamHi + NsiI, which was identified from a pilot study designed to target ~5000 marker loci. The combined libraries were then pooled and sequenced on a NextSeq 1 × 150-bp run. Reads were assessed for quality control and demultiplexed. We then removed facility-specific adapter sequences (See Data S1 for more detailed methods). We aligned reads and called SNPs using the Stacks 2.59 de novo pipeline and *populations* function (see Data S1 for more details on sequence analyses; Catchen et al., 2011; Rochette et al., 2019). We included loci that were present in at least 70% of individuals, and all individuals were genotyped at >60% of loci (mean number of missing loci per individual: 19.6%). Our final dataset included 3690 loci, of which 3071 were polymorphic (Figures S4 and S5).

2.3 | Landscape genetic analysis

All analyses were conducted in the R v. 4.1.1 (R Core Team, 2021) unless otherwise noted.

2.3.1 | Isolation by distance

We tested for IBD using a Mantel test of the correlation between genomic and geographic distance. Genomic distance was calculated using Nei's *D* with the 'dist.genepop' function in the package 'adegenet' (Jombart, 2008; Jombart & Ahmed, 2011); geographic distance was calculated using the 'rdist.earth' function in the package 'fields' (Nychka et al., 2021). We tested whether the observed correlation was greater than random expectation using a permutation test with 999 permutations.

We also determined the geographic distance at which the IBD correlation was maximized using the 'dist_max_corr' function from the 'graph4lg' package (Savary et al., 2020). The function uses an expanding window to calculate the correlation coefficient for pairs with geographic distances that fall within a set range for 1000 sequential range intervals from 0 to 659 km.

2.3.2 | Principal components and spatial principal components analyses

We conducted genetic principal components analysis using the function 'dudi.pca' from the package 'ade4' (Bougeard & Dray, 2018; Chessel et al., 2004; Dray et al., 2007; Dray & Dufour, 2007; Thioulouse et al., 2018). Principal components describe the major axes of genetic variation and cluster individuals that have similar genotypes (Abegaz et al., 2019; Novembre & Stephens, 2008; Reich et al., 2008).

We also conducted spatial principal components analysis (sPCA), which is a spatially explicit ordination. The method accounts for both genetic variation (PCA) and spatial autocorrelation (Moran's *I*; Jombart et al., 2008). The PCA was calculated as above using allele frequencies and spatial autocorrelation using a neighbourhood weighting matrix describing the spatial proximity of samples. We calculated neighbourhood weights using a Gabriel graph (Matula & Sokal, 2010; Figure S6). Large positive eigenvalues of sPCA describe global patterns of spatial variation where there is both high genetic variation and high values of Moran's *I* (i.e. physically close samples are also most similar genetically). Large negative eigenvalues describe local patterns of genetic structure (i.e. physically closer samples are more genetically dissimilar). These analyses were conducted with the 'spca' function in the package 'adegenet' (Jombart, 2008; Jombart & Ahmed, 2011).

We tested for the overall significance of global and local genetic patterns using the 'global.rtest' and 'local.rtest' permutation tests in 'adegenet'. These tests determine whether the maximum correlation between allele frequency and global (positive) or local (negative) Moran eigenvector maps (MEMs) computed for the sample Gabriel graph is greater than random expectation (Jombart et al., 2008). A significant result indicates that there was at least one sPCA axis that described significant spatial structure in genetic variation. We then used the 'screeplot' function to visualize the relative importance of sPCA eigenvalues. The function generates a screeplot and a histogram to determine which axes to further examine (Jombart et al., 2008). We visualized eigenvalues that were disjunct from the majority in the screeplot and histogram (Jombart et al., 2008).

2.3.3 | ConStruct analysis

We used conStruct to determine whether there were areas of discrete population structure, which may indicate an environmental influence on invasive spread, while accounting for potentially continuous IBD (Bradburd et al., 2018). We calculated cluster assignments for $K = 1–6$ within both a spatial framework (i.e. accounting for continuous IBD) and in a non-spatial framework (i.e. where the spatial element in the conStruct model was set to 0, which is similar to a traditional STRUCTURE analysis; Pritchard et al., 2000). We used the 'conStruct' function from the package 'conStruct' and ran each model for 250,000 iterations and visualized trace plots of chains to ensure proper convergence and mixing (Bradburd, 2019). We calculated layer contributions and determined the most supported number of clusters as occurring when the contribution of an additional layer was less than 5% (Bradburd et al., 2018). We corroborated clustering patterns using fineRADstructure (Malinsky et al., 2018; See Data S1 for fineRADstructure methods and results; Figure S22).

2.3.4 | Effective migration surfaces

We examined whether IBD was spatially heterogeneous using Fast Estimation of Effective Migration Surfaces (FEEMS; Marcus et al., 2021; Petkova et al., 2016). The model generates expected genetic distances between populations, which approximate the resistance to gene flow between the populations (Marcus et al., 2021; Petkova et al., 2016). Weights (w) along edges in the grid are then assigned, which represent effective migration. We were particularly interested in determining geographic regions where putative gene flow was high as well as areas that posed distinct barriers to movement. FEEMS has the capacity to handle sparse grids with anisotropic migration between nodes, which were present in our spatial dataset.

We constructed a triangular discrete digital global grid (~100 km^2/triangle) across the state of Minnesota using the package 'dggridR' (Barnes & Sahr, 2021). Each sample was associated with the closest node in the grid (Figure S7). The 176 samples were associated with 146 nodes. At grid nodes assigned more than one sample, we calculated allele frequencies based on the combined genetic information. The allele frequency dataset was converted to plink format using plink 1.9 (Purcell, 2019; Purcell et al., 2007) using plink ready files exported from Stacks 2.59 *populations* function (see above).

Effective migration surface models included a regularization term that penalized large differences in weights between adjacent nodes and was controlled by the smoothing parameter, λ. We used a 'leave-one-out' cross-validation procedure (i.e. 146-folds that leave a node out of estimation and used it for calculation of the loss function) to determine the most appropriate value of λ. We tested 20 models using logarithmically spaced lambda values between $1e^{-6}$ and $1e^{2}$ and chose the model with a λ value that minimized the mean L2 error (Marcus et al., 2021).

2.3.5 | Environmental data

We analysed environmental datasets on climate, soils and land use (Table S2; See Data S1 for more detailed descriptions of environmental variables). All environmental data were downloaded in or reprojected onto WGS84 with a resolution of 30 arc seconds (~1 km resolution). For climate, we focused on three bioclimatic variables from the WorldClim dataset (worldclim.org) that show the strongest gradients across Minnesota: mean temperature of the warmest quarter (Bio 10), minimum temperature of the coldest month (Bio 6) and precipitation in the warmest quarter (Bio 18; Figures S8 and S9). These variables have been shown to be relevant to plant establishment and growth across systems (Briscoe Runquist et al., 2021; Chapman et al., 2017; 2019; Gorton et al., 2019; Petitpierre et al., 2017; Wolkovich et al., 2012). In a PCA of all bioclimatic variables (Table S3), the three variables were not strongly correlated (Table S4) and were representative of major axes of environmental variation for the first three PCs (Figure S8 and Table S5; See Data S1 for detailed PCA of all bioclimatic variables).

For soils, we sourced data at ~1 km resolution from the International Soil Reference Information Center (https://files.isric.org/soilgrids/latest/data_aggregated/1000m/) and USDA NRCS

Soils gNATSGO database (www.nrcs.usda.gov), which is the finest resolution available for those data. Due to the large number of potential soil variables, we performed separate PCAs for soil composition and chemistry variables in order to produce composite variables that describe major axes of variation: soil composition (variables: bulk density, coarse fragment volume, volumetric water content at 33 kPa, available water storage, and clay, silt and sand composition; Figure S10 and Table S6) and soil chemistry (variables: cation exchange capacity, nitrogen content, soil organic carbon content, soil organic carbon density and pH of soil water; Figure S11 and Table S6). We retained the first two PCs from each PCA [Soil Comp PC1 (48.4% variation), Soil Comp PC2 (20.5% variation), Soil Chem PC1 (36.6% variation) and Soil Chem PC2 (29.1% variation); (Figures S10 and S11)]. We included soil drainage classification (seven classification categories ranging from very poorly drained to excessively drained; Figure S12 and Table S7).

To characterize anthropogenic factors, we downloaded a land use classification map (15 classification categories; USGS National Land Cover Database for 2019; Figure S13 and Table S8) and the percent impervious surface coverage (Multi-resolution Land Characteristic Consortium, https://www.mrlc.gov/).

2.3.6 | Isolation by environment

We used the environmental data to generate environmental resistance surfaces with the R package 'ResitanceGA' (Peterman, 2018). This package uses a genetic algorithm to optimize the relationship between genetic chord distances and a resistance transformation of the environmental data. More specifically, the package first generates multiple resistance models using non-linear transformations (e.g. monotonic or Ricker model) of the environmental distance data (i.e. generate putative environmental resistance functions) and then calculates their corresponding estimates of landscape resistance using CircuitScape implemented in Julia (Anantharaman et al., 2020). The models are allowed to compete and the best-performing models, as determined by the Akaike information criterion with small sample size correction (AICc), are kept and parameters are mutated for the next iteration (e.g. small perturbations to the original model parameter combinations). The algorithm runs until 25 consecutive iterations do not yield a significant improvement in model fit, and the optimized parameter estimates of the best model are then used for further analyses.

To test for IBE, we optimized resistance surfaces for each environmental layer individually in 'Resistance GA' analyses. Each run of 'ResistanceGA' also estimates a null geographic distance model. To examine whether particular environmental variables generated IBE, we compared the optimized environmental resistance model to the null model (using ΔAICc). This allowed us to determine whether the inclusion of environmental resistance significantly improved model fit. We projected the resulting resistance model surfaces and compared model metrics for each environmental variable.

To determine which environmental resistance variables were the most strongly associated with genetic distance, we used multiple regression on distance matrices (MRDM) (Balkenhol et al., 2009; Legendre et al., 1994). We included resistance matrix outputs from optimized CircuitScape models (i.e. for individual environmental models) as independent variables and genetic chord distance as the dependent variable. We included geographic distance as a null independent variable (Dyer et al., 2010). We standardized all optimized resistance layers to mean zero and standard deviation one. Evaluating resistance layers using Circuitscape and MRDM determines which environmental factors best explain patterns of genetic distance across the landscape and potentially drive IBE (Peterman & Pope, 2021). Models were run using the 'MRM' function in the package 'ecodist' (Goslee & Urban, 2007).

While useful for investigating IBE, MRDM analyses do not necessarily describe the realized pathways of movement across a landscape, which may depend on multiple and/or non-linear interactions among environmental factors that are not included in the individual environmental ResistanceGA optimizations. To determine the overall landscape patterns of movement, we also optimized a multi-environmental factor resistance surface model that included all environmental layers in a ResistanceGA model and allowed for interactions among environmental variables in the non-linear transformations. The resulting resistance matrix is most likely to describe composite environmental IBE and how pathways of movement are influenced by the aggregate effects of environmental variables. Due to the large number of environmental variables included in this model, we executed three independent runs of ResistanceGA to check for model stability and averaged across individual results.

2.4 | Ecological niche analysis

We tested for niche differentiation between clusters identified by the spatially explicit conStruct results using the 'ecospat' package (Di Cola et al., 2017). We defined the available environmental background space using 1000 randomly generated points drawn from a spatial polygon of Minnesota. We investigated niche differences for the full set of environmental variables (climate, soil and anthropogenic, *heretofore*: aggregate environmental variables) and for climate variables, alone. For the aggregate environmental variables, we conducted an Hill-Smith ordination (ordination of tables mixing quantitative variables and factors; Hill & Smith, 1976) for background and sample points using the function 'dudi.hillsmith' from the 'ade4' package. We retained the first three axes of variation for niche analyses. For the climate variables, we conducted a principal component analysis using the 'dudi.pca' function from the package 'ade4' and retained the first two axes.

We quantified four measures of niche differentiation. We quantified niche overlap using Schoener's *D*, which accounts for both breadth and density and varies between 0 and 1 (zero and complete niche overlap, respectively). We also calculated what proportion of the combined niche space represented niche stability, expansion and unfilling. Niche stability is the proportion of niche that overlaps, niche expansion is the proportion of the Cluster 2 niche that does not overlap Cluster 1,

and niche unfilling is the proportion of Cluster 1 that does not overlap Cluster 2. We tested for niche equivalency using a permutation test ($n=999$; i.e. within the niche space of common tansy, do assigned clusters overlap less than would be expected by chance?). All tests were one-tailed. We tested the hypothesis that overlap, stability and unfilling were less than random expectation and that expansion was greater than random expectation.

3 | RESULTS

3.1 | Landscape genetic analyses

3.1.1 | Isolation by distance

We did not detect evidence of IBD using a parametric test ($r=.06$, $p=.1$) or when we used loess to explore the relationship at varying distances (Figure 2a). Isolation by distance was highest at 108 km ($r=.14$, Figure 2b); however, the IBD correlation coefficient was similar across the range of distances ($r=.08$–$.13$ for distances of 150–660 km).

3.1.2 | Principal components analysis

The first three axes of the PCA accounted for 7.6% of genetic variation (PC1: 3.6%, PC2: 2.1%, PC3: 1.9%). Axis 1 and Axis 3 had high spatial autocorrelation (Axis 1: Moran's $I=0.48$, $p<.001$; Moran's $I=0.27$, $p<.001$); whereas Axis 2 had moderate spatial autocorrelation (Moran's $I=0.10$, $p=.034$).

The far northwestern and several northeastern samples separated from the rest along PC1 (Figures 2c,e and S14). Two samples from the northwest and two from the southwest separated from the remainder along PC2 (Figures 2c,f and S14). Northwestern and northeastern samples occupied largely overlapping but offset areas along PC3 (Figure S15). Otherwise, we did not detect population structure based on subsequent axes.

3.1.3 | Spatial principal components analysis

We found a significant global spatial structure: geographically proximal populations had more similar allele frequencies than random expectation (permuted statistic = 0.009, $p=.01$; Figure S16). By contrast, we found no evidence for local spatial structure: neighbouring populations did not have more dissimilar allele frequencies than random expectation (simulation statistic = 0.007, $p=.85$; Figure S16).

The first three global sPCA axes (i.e. positive) were distinct from the rest in diagnostic plots (Figure S17), represented substantial genetic variance and had high spatial autocorrelation (Tables 1 and S9). Axis 1 separated most far northwestern samples (Red River Prairie/Aspen Parklands/Agassiz Lowlands) from the remaining samples (Figures 2d and S14). Axis 2 separated most northeastern samples from the remainder, particularly those from the north shore of Lake Superior (Figures 2d and S14). Axis 3 further supported the differentiation of far northwestern and northeastern samples from the remainder (Figure S18).

We found a strong correlation between PC1 and sPC1 ($r=-.70$; $p<.001$) and moderate correlations between PC2 and sPC3 ($r=-.35$; $p<.001$) and PC3 and sPC2 ($r=-.46$; $p<.001$). Correlations between all other combinations were weak ($r<.12$; $p<.05$; Table S10).

3.1.4 | ConStruct analysis

The conStruct analysis supported $K=4$ and $K=2$ as the most probable number of clusters for the non-spatial and spatial analyses, respectively (Figures 3 and S19–S21). Both analyses revealed similar patterns of population structure as PCA and sPCA analyses (Figure 3).

In the non-spatial analysis, far northwestern samples (Red River Prairie/Aspen Parklands/Agassiz Lowlands) were differentiated from the remaining samples; far northwestern samples were assigned primarily to one cluster and had low proportions of the other clusters (lilac cluster; Figure 3a,b). The remainder of the samples had more variable cluster proportions. The remaining northwestern and southwestern samples had higher proportions of a second cluster (burgundy cluster; Figure 3a,b) compared with northeastern individuals, which had higher proportions of a third cluster (teal cluster; Figure 3a,b). The remaining cluster was found in low proportion across the regions with some notable exceptions in individuals from the south (yellow cluster; Figure 3a,b).

Spatial autocorrelation and continuous IBD in genetic samples may inadvertently suggest discrete population structure that is not a true representation of demographic processes. The spatial conStruct analysis can account for these continuous relationships while generating cluster assignments. In the spatial analyses, cluster assignments were similar to the non-spatial analysis but more clearly demarcated individuals from far northwestern MN. These samples were predominantly assigned to one cluster and had very low proportions of the other clusters (light blue cluster; Figure 3c,d). There was also a small region of northeastern MN (North Shore Highlands/Laurentian Uplands) where individuals had higher proportions of this cluster. The remaining individuals were primarily assigned to the alternate cluster (dark berry cluster; Figure 3c,d).

3.1.5 | Fast estimated effective migration surfaces

FEEMS identified two areas with reduced effective migration (Figure 4). There was a particularly pronounced area of reduced effective migration surrounding far northwestern populations. The area of lowest effective migration separated northwest populations from north-central populations (Aspen Parklands/Red River Prairie/Agassiz Lake from Chippawa Plains/Hardwood Hills; Figure 4). This boundary aligned geographically with groupings identified by

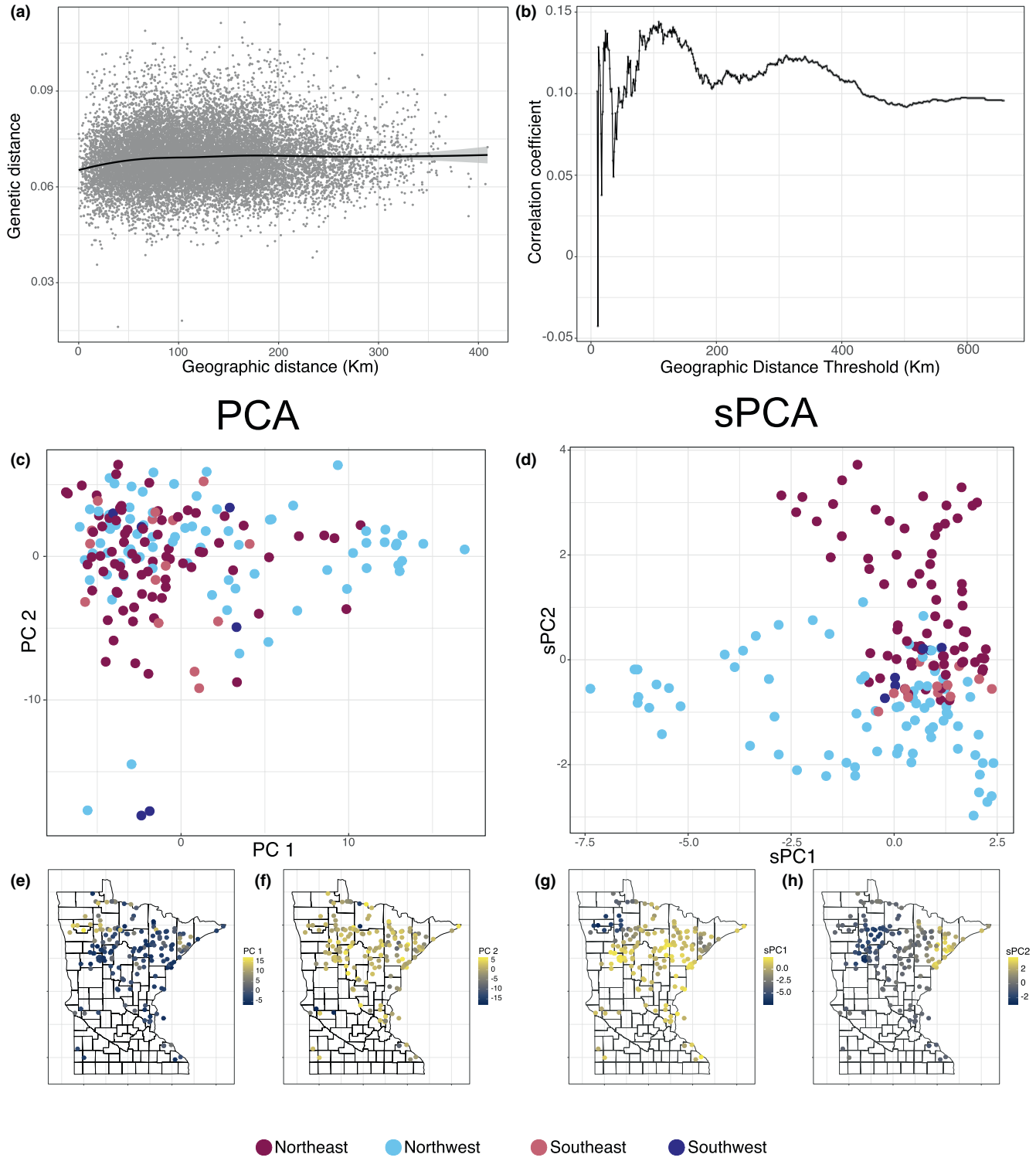

FIGURE 2 (a) Relationship of genetic distance (Nei's *D*) and geographic distance for pairs of populations to test for isolation by distance. Fit is shown by loess. (b) The Mantel correlation statistic between population pairs for genetic distance and geographic distance when (y-axis) calculated using an expanding window of distances to calculate correlation. (c) Principal components analysis (PCA) biplot of the first two PCs. Samples are coloured by the quadrant of MN from which they originated: northeast (dark berry-purple), northwest (light blue), southeast (light berry-pink) and southwest (dark blue). (d) Spatial PCA biplot of the first two positive sPCA axes. Colours are the same as for PCA. (e–h) Geographic pattern of PCs and sPCA axes. Dark blue indicates lower values and light yellow indicates higher values. (e) PC1. (f) PC2. (g) sPC1. (h) sPC2.

PCA, sPCA and conStruct. In northeastern MN, there was reduced effective migration among a group of populations in the middle of the region (North Shore Highlands/Laurentian Uplands). Southern MN had greater variation compared with other areas of the state in effective migration rates. Conversely, effective migration was relatively high among populations in north-central and northeastern MN (Figure 4).

The model with lambda = 0.1128 had the lowest L2 cross-validation error (Figure S23) and was used to calculate and visualize the effective migration surface (Figures 4 and S24). Additionally, we found models using a range of lambda values identified similar geographic patterns of reduced migration (Figure S24).

TABLE 1 Eigenvalues of the first three global sPCA axes and their decomposition into genetic variance and Moran's *I* values.

Axis (λ) number	Eigenvalue	Genetic variance	Moran's *I*
λ1	4.0	24.3	0.66
λ2	2.0	10.4	0.76
λ3	1.8	10.6	0.67

3.1.6 | CircuitScape

We calculated resistance surfaces for environmental factors individually and in combination. When analysed individually, the inclusion of any environmental variable improved model performance

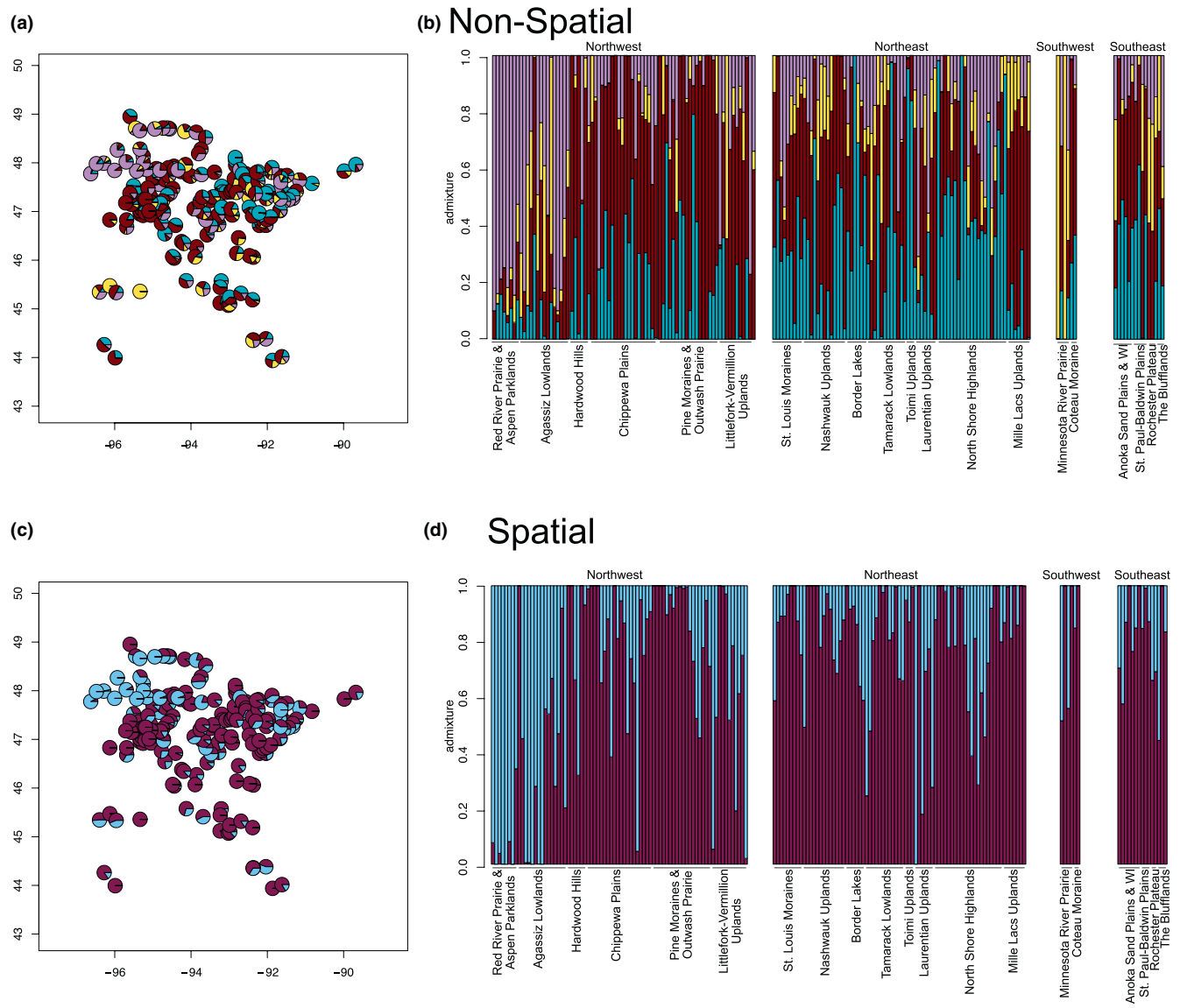

FIGURE 3 Non-spatial and spatial conStruct analyses. (a, b) $K = 4$ from the non-spatial conStruct analysis. Clusters 1, 2, 3 and 4 are shown in lilac, burgundy, teal and yellow, respectively. (c, d) $K = 2$ from the spatially explicit conStruct analysis. Clusters 1 and 2 are shown in light blue and dark berry-purple, respectively (a, c) Spatial view of cluster assignment where each pie chart shows the fraction of each cluster. (b, d) STRUCTURE barplot view of conStruct assignments. Each bar represents a sample and the bar proportion represents the cluster assignment fraction. Bars are clustered by hierarchical geography, first within their MN quadrant and then within the ecological subsection.

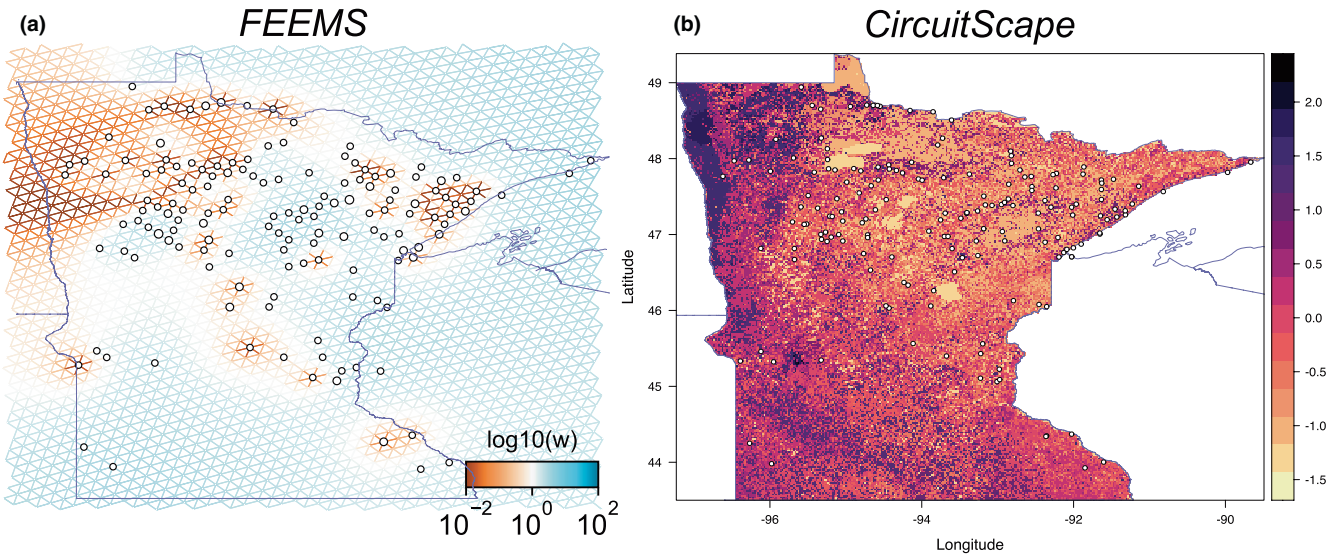

FIGURE 4 Effective migration and resistance to gene flow of common tansy across Minnesota. (a) Fast Estimation of Effective Migration Surface (FEEMS) of common tansy in Minnesota. White points represent nodes with assigned samples and edges denote potential paths of travel. Edges coloured blue have higher effective migration and edges coloured brown have less effective migration. (b) Multivariable environmental resistance surface estimated using CircuitScape. The projection is the average of three model runs. Darker purple colours indicate greater resistance values; lighter cream and orange colours indicate lower resistance. Small white circles with black outlines represent sampling sites.

compared with a model that included only distance. However, land classification, minimum temperature of the coldest month, precipitation of the warmest month and soil chemistry PC1 resulted in the most substantial gains to model performance ($\Delta AIC < -100$ & marginal $R^2 > .20$; Table S11). Including per cent impervious surface in a resistance model resulted in moderate performance gains ($\Delta AIC = -45.4$ & marginal $R^2 = .07$; Table S11). Geographic distance, alone, explained only 2% of the variation (marginal R^2).

The following environmental factors had the greatest influence on genetic distance. Croplands, grasslands and managed developed areas (e.g. parks) had the highest resistance values compared with pastures, low to moderately developed areas and mixed forests, which had the lowest resistance values (Table S12, Figure S25). For climate variables, areas with the coldest temperatures had higher resistance and areas with the lowest and highest precipitation had higher resistance (Table S12, Figure S25). Areas of very high and low values of soil chemistry PC1 (high pH or high nitrogen) had higher resistance (Table S12, Figure S25). Last, areas with high percentages of impervious surface had less resistance to gene flow than areas with less impervious surface (Table S12, Figure S25).

In the MRDM analysis, genetic distance had a significant or nearly significant relationship with geographic distance, soil variables and land use (Table S13). Higher resistance was associated with both soils that are poorly and excessively drained and soils that have higher organic matter. Highly cultivated areas also had very high resistance values.

In the multi-surface CircuitScape models, the composite resistance surfaces indicated less resistance to gene flow in northeastern and north-central Minnesota compared with the northwest (Figures 4b and S26). Areas of low gene flow identified by CircuitScape were consistent with the FEEMS migration surface (Figure 4a,b). Replicate CircuitScape model optimizations were largely consistent across the three independent runs. The three models explained between 12.0% and 26.4% of the variation in genetic distance (marginal R^2). Across all three models, the environmental factors that consistently had the strongest explanatory relationships with gene flow were land use classification (24.7%–46.4% contribution), soil drainage class (10.7%–24.3%) and precipitation of the warmest quarter (7.8%–27.5%; Table S14).

3.2 | Ecological niche analysis

In the ordination of aggregate environmental variables (climate, soil and anthropogenic), the first three axes accounted for approximately 30% of variation (Axis 1: 15.0%; Axis 2: 7.9%; Axis 3: 5.8%). The first axis described the environmental gradation that distinguishes northern and southern regions of the state and was defined by temperature, soils drainage and forest cover. Axis 2 primarily separated eastern and western regions of the state and was defined by differences in precipitation and forest cover. Axis 3 was primarily associated with the degree of development in an area (Figure S27; See Data S1 for more details). In the principal components analysis of climate variables, the first two principal component axes accounted for 96.5% of the variation (PC1: 61.6%; PC2: 35.0%). PC1 described mainly temperature; PC2 described mainly precipitation (Figure S28).

The two main clusters identified by the spatially explicit conStruct analysis occupy overlapping ecological niches for both the

aggregate environmental variables and climate variables (Figure 5; Cluster 1: dark berry; Cluster 2: ice blue; overlap: yellow). Based on aggregate environments, Cluster 1 included environments that were colder and drier than those occupied by Cluster 2 with moderately to poorly drained soils (Figure 5a–c). Based on climate alone, Cluster 1 occupied cooler and drier environments (Figure 5d; Cluster 1: burgundy; Cluster 2: teal; overlap: lilac). The non-overlapping sections of the aggregate and climate niche for Cluster 1 represented significant niche expansion when compared to Cluster 2; permutation tests for Schoener's *D*, niche stability and niche expansion all indicated differences from random expectation (Table 2). The niche differences we found are consistent with a niche shift concurrent with the timeline of range expansion into northwestern MN.

4 | DISCUSSION

The role of environmental variation in modulating invasion dynamics and population genomic structure across landscapes remains unclear (Cruzan & Hendrickson, 2020). In this study, we took advantage of a recent range expansion to dissect the relative influences of distance and environmental factors on landscape genomic structure. We found evidence for IBE but no evidence for IBD. Land use and soils had particularly strong influences on fine-scale structure. Our results also suggested that genotypes from a recently invaded area exhibit genomic divergence and occupy a novel set of environments relative to the rest of the region. These results suggest that range shifts with climate change may be affected by the interactive

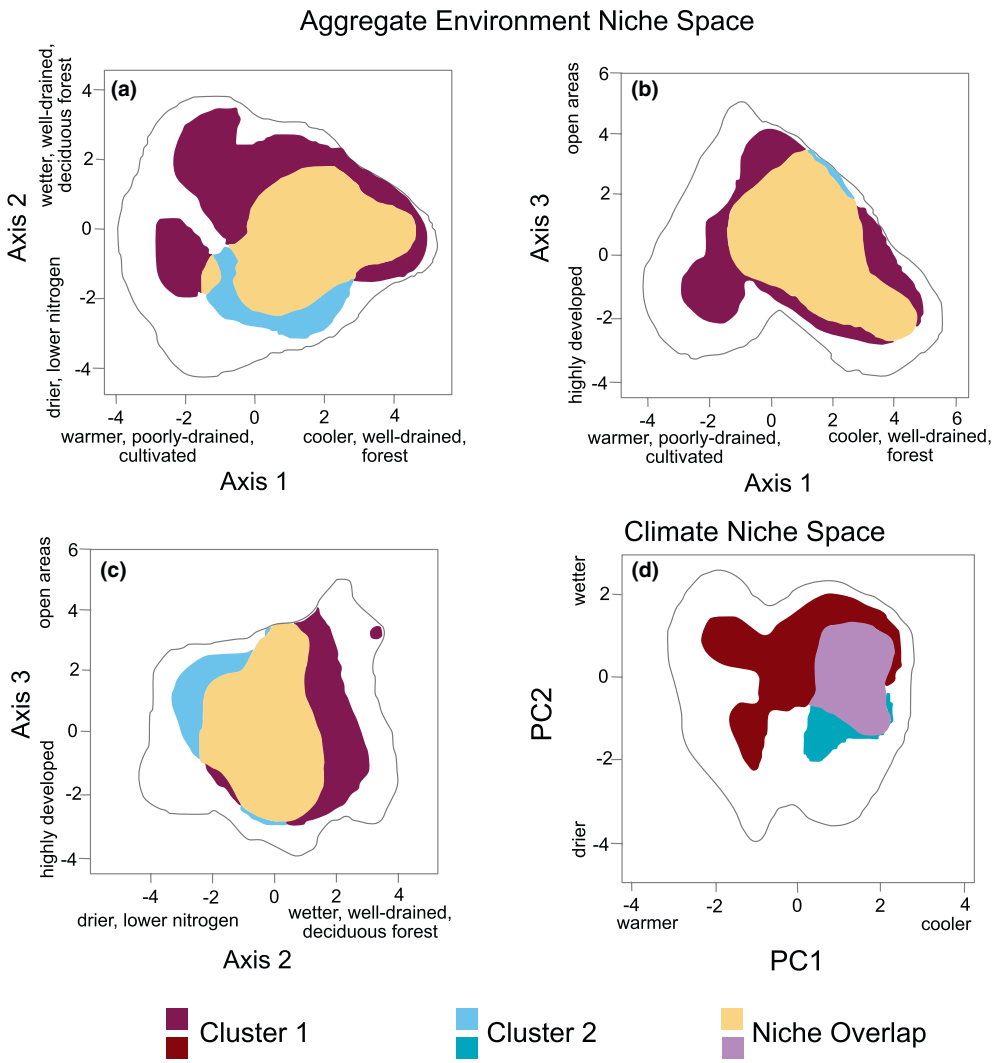

FIGURE 5 Ecological niche of common tansy genetic clusters. (a–c) Niche space based on all environmental variables used in the paper. Dark Berry colour represents the exclusive niche space of Cluster 1; ice blue represents the exclusive niche space of Cluster 2; yellow represents the niche space overlap for Cluster 1 and Cluster 2. The grey outline surrounds the total available niche space in Minnesota. (a) Biplot of niche space for mixed ordination Axis 1. (b) Biplot of niche space for mixed ordination Axes 1 and 3. (c) Biplot of niche space for mixed ordination Axes 2 and 3. (d) Principal components climatic niche space. Burgundy represents the exclusive niche space of Cluster 1; teal represents the exclusive niche space of Cluster 2; lilac represents the niche space overlap for Cluster 1 and Cluster 2. The grey outline surrounds the total available niche space in Minnesota.

TABLE 2 Environmental niche equivalency tests for aggregate environmental variables and climatic variables.

	Aggregate environmental niche						Climatic niche	
Metric	Statistic (Axes 1 and 2)	*p*	Statistic (Axes 1 and 3)	*p*	Statistic (Axis 2 and 3)	*p*	Statistic (Axes 1 and 2)	*p*
Schoener's *D*	**0.47**	**.008**	0.69	.63	0.40	.08	**0.39**	**.004**
Stability	**0.82**	**.002**	0.99	**.81**	**0.81**	**.002**	**0.85**	**.03**
Expansion	**0.18**	**.002**	0.00	**.81**	**0.19**	**.002**	**0.14**	**.03**
Unfilling	0.25	.902	0.12	.51	0.24	.876	0.34	.98

All bolded values are $p < .05$.

effects of environmental variables on patterns of movement across landscapes.

There was little evidence of IBD regardless of the spatial scale that we examined. This pattern suggests that migration was not consistent with a stepping-stone model and that invasion did not always occur via geographically nearest neighbours. IBD is often reduced or absent in population genetic studies of invasive species (Hutchison & Templeton, 1999; Moyle, 2006; Slatkin, 1993). For example, in a global analysis of the genus *Silene*, invasive species showed no evidence for IBD but native species often exhibited IBD (Moyle, 2006). A lack of IBD may occur due to historical introduction effects, rapid expansion, stochastic long-distance dispersal or environmentally mediated migration (Bradburd & Ralph, 2019; Duforet-Frebourg & Blum, 2014) and all have been found in invasive species (Dlugosch & Parker, 2008; Lake et al., 2023; Leblois et al., 2000; Lu et al., 2022; Schlaepfer et al., 2008). We also investigated IBD at fine spatial scales using loess and found some evidence for elevated correlations between geographically proximal samples. In PCA, sPCA and construct analyses, geographically proximal samples were also more similar but there was little evidence for broad geographic structure (Figures 2 and 3). Last, FEEMS identified fine-scale geographic pockets of high effective migration separated by distinct areas of low effective migration (Figure 4). Together, these results are consistent with a history of recent expansion and a departure from migration–drift equilibrium.

Although range expansion has been recent and rapid, environmental factors shaped movement of common tansy across Minnesota. Although tests for IBE are uncommon for invasive plants (Cruzan & Hendrickson, 2020; Etherington, 2015; but see Alvarado-Serrano et al., 2019), our findings are consistent with other recent studies (Alvarado-Serrano et al., 2019; Hofmeister et al., 2021; Ray & Ray, 2014; Yang et al., 2020). In these studies, climate and land use most often influenced spatial patterns of population genetic structure. However, most studies assessed vagile species, broader geographic areas or focused on adaptive evolution. Our fine-scale sampling of a recent invasion suggests that IBE influenced range expansion—all environmental variables had stronger relationships with genetic distance than geographic distance (Table S11). Identification of the environmental factors and the scales over which they operate will allow for better identification of regions at the highest risk of future invasion.

Land use and soil variables had the greatest influence on landscape genetic patterns in common tansy, but they operated at different spatial scales. Patterns of resistance for land use echoed large-scale patterns of recent range expansion (Figure S25). The lowest resistance to gene flow was found in disturbed/barren, moderately developed, and pastures of northeastern and central MN. Conversely, the highest areas of resistance were found in heavily cultivated and grassland ecosystems in southern and western MN. These results suggest that invasion occurred along corridors of disturbance and rangeland but outside of intensive cropping systems, which is common for invasive plants (reviewed in Theoharides & Dukes, 2007). Soils were an important determinant of IBE at smaller geographic scales. Across the different CircuitScape analyses, high resistance to gene flow was associated with high pH, high nitrogen, poorly drained and excessively drained soils, and soils with high organic matter. Investigating the mechanisms underlying the differences in resistance, particularly among different agricultural land uses (e.g. rangeland versus cropland), may help management efforts to stem further range expansion. Identifying major causes of resistance across landscapes can inform predictions of range shifts with climate change. Range shifts are modulated by the distribution of suitable climate and the potential for movement from unsuitable to suitable areas. Insights from population genomics about historical barriers to movement can inform migration models used to predict future range shifts with climate change (e.g. Prasad et al., 2020).

Several analyses identified a genetically distinct group of samples from far northwestern MN (Aspen Parklands/Red River Prairie and a portion of the Agassiz Lowlands). These samples were distinct from other regions along both PC1 and sPCA Axis 1, had high admixture proportions of a single genetic cluster assignment and were separated geographically by an area of reduced effective migration in the FEEMS analysis (Figures 2–4). These samples are from an expanding range margin that is still sparsely populated, and the vast majority of occurrence records are dated from 2010 to the present (EDDMapS, 2023). Land managers from this region have also noticed a very recent increase in westward expansion. Genetically, the samples from this area are most like a small group of samples from the centre of the northeastern region and along the northern border (i.e. ice blue cluster in spatial conStruct analysis; Figure 3). The clustering and IBE results suggest that colonization did not occur via the most direct geographic path and likely occurred though dispersal along more favourable environments. In addition, the realized

niche of the conStruct cluster that included the far northwestern populations occupied a slightly different portion of environmental space that is outside of the historical environmental niche of common tansy. This result suggests that the full range of suitable environments may not yet be occupied or that adaptive evolution has facilitated recent invasion. Experimental work is needed to explicitly test for adaptive evolution at range margins and distribution models incorporating adaptative evolution are needed to refine predictions of invasion risk.

Isolation by environment was more likely to explain landscape genomic differentiation of common tansy indicating that environmental factors helped shape recent and rapid range expansion. Our results add to a growing body of research showing that invasion often does not occur strictly via wave-like spread but is modulated by climate, land use and soils. Using fine-scale regional sampling, we were able to demonstrate that environmentally mediated gene flow was also scale-dependent with different environmental factors influencing movement at different scales. Long-term management will need to account for these complex interactions of environmental factors to halt further range expansion, especially in the face of continued global change. Moreover, the results indicate that adaptation to leading-edge environments may facilitate range expansion and that predictive models of future habitat suitability should account for such adaptive differentiation.

AUTHOR CONTRIBUTIONS

RBR and DM conceived of and designed the research study. RBR collected samples and performed the research. RBR performed the analyses and drafted the paper. RBR and DM both contributed substantially to the editing and final version of the paper.

ACKNOWLEDGEMENTS

We thank T. Lake for help with sample collection and B. Greene and D. Schoenecker for help with sample organization and preservation. We thank T. Lake, R. Venette, Y. Brandvain and L. Flagel for thoughtful conversations about analyses. We thank the natural resources community for helpful conversations about common tansy invasion, including G. Foltz (Clay Co. SWCD), M. Watland (Becker Co. SWCD), MN Department of Natural Resources, in particular, A. Danielson and S. Pennington and L. Van Riper, and MN Department of Agriculture, in particular T. Cortilet. Funding for this project was provided by the Minnesota Invasive Terrestrial Plants and Pests Center through the Environment and Natural Resources Trust Fund as recommended by the Legislative-Citizen Commission on Minnesota Resources (LCCMR).

CONFLICT OF INTEREST STATEMENT

The authors declare no conflicts of interest.

DATA AVAILABILITY STATEMENT

Raw sequence reads are deposited in the SRA (BioProject PRJNA1099706 SUB14375599). Individual genotype data are archived and available through UMN DRUM: https://doi.org/10.13020/nx0n-f098 and Dryad: https://doi.org/10.5061/dryad.h70rxwdsk. All additional data, metadata and scripts are available at github/rdbrunquist/common-tansy-landscape genomics.

BENEFIT-SHARING STATEMENT

Benefits from this research accrue from the sharing of our data and results on public databases as described above.

ORCID

Ryan Briscoe Runquist https://orcid.org/0000-0001-7160-9110
David A. Moeller https://orcid.org/0000-0002-6202-9912

REFERENCES

Abegaz, F., Chaichoompu, K., Génin, E., Fardo, D. W., König, I. R., Mahachie John, J. M., & van Steen, K. (2019). Principals about principal components in statistical genetics. *Briefings in Bioinformatics*, *20*, 2200–2216.

Alvarado-Serrano, D. F., Van Etten, M. L., Chang, S.-M., & Baucom, R. S. (2019). The relative contribution of natural landscapes and human-mediated factors on the connectivity of a noxious invasive weed. *Heredity*, *122*, 29–40.

Anantharaman, R., Hall, K., Shah, V. B., & Edelman, A. (2020). Circuitscape in Julia: High performance connectivity modelling to support conservation decisions. *JuliaCon Proceedings*, *1*, 58.

Atwater, D. Z., & Barney, J. N. (2021). Climatic niche shifts in 815 introduced plant species affect their predicted distributions. *Global Ecology and Biogeography*, *30*, 1671–1684.

Atwater, D. Z., Sezen, U. U., Goff, V., Kong, W., Paterson, A. H., & Barney, J. N. (2016). Reconstructing changes in the genotype, phenotype, and climatic niche of an introduced species. *Ecography*, *39*, 894–903.

Baker, H. G., & Stebbins, G. L. (Eds.). (1965). *The genetics of colonizing species*. Academic Press.

Balkenhol, N., Waits, L. P., & Dezzani, R. J. (2009). Statistical approaches in landscape genetics: An evaluation of methods for linking landscape and genetic data. *Ecography*, *32*, 818–830.

Barnes, R., & Sahr, K. (2021). dggridR: Discrete Global Grids. https://github.com/r-barnes/dggridR/

Barrett, S. C. H. (2015). Foundations of invasion genetics: The Baker and Stebbins legacy. *Molecular Ecology*, *24*, 1927–1941.

Bougeard, S., & Dray, S. (2018). Supervised multiblock analysis in R with the ade4 package. *Journal of Statistical Software*, *86*, 1–17.

Bradburd, G. (2019). conStruct: Models Spatially Continuous and Discrete Population Genetic Structure. R package version 1.0. 4.

Bradburd, G., Ralph, P., & Coop, G. (2013). Disentangling the effects of geographic and ecological isolation on genetic differentiation. *Evolution*, *67*, 3258–3273.

Bradburd, G. S., Coop, G. M., & Ralph, P. L. (2018). Inferring continuous and discrete population genetic structure across space. *Genetics*, *210*, 33–52.

Bradburd, G. S., & Ralph, P. L. (2019). Spatial population genetics: It's about time. *Annual Review of Ecology, Evolution, and Systematics*, *50*, 427–449.

Briscoe Runquist, R. D., Lake, T. A., & Moeller, D. A. (2021). Improving predictions of range expansion for invasive species using joint species distribution models and surrogate co-occurring species. *Journal of Biogeography*, *48*, 1693–1705.

Catchen, J. M., Amores, A., Hohenlohe, P., Cresko, W., & Postlethwait, J. H. (2011). Stacks: Building and genotyping loci de novo from short-read sequences. *G3: Genes – Genomes – Genetics*, *1*, 171–182.

Chapman, D., Pescott, O. L., Roy, H. E., & Tanner, R. (2019). Improving species distribution models for invasive non-native species

with biologically informed pseudo-absence selection. *Journal of Biogeography*, *46*, 1029–1040.
Chapman, D. S., Scalone, R., Štefanić, E., & Bullock, J. M. (2017). Mechanistic species distribution modeling reveals a niche shift during invasion. *Ecology*, *98*, 1671–1680.
Chessel, D., Dufour, A. B., & Thioulouse, J. (2004). The ade4 package - I: One-table methods. *R News*, *4*, 5–10.
Clasen, B., Moss, N., Chandler, M., & Smith, A. (2011). A preliminary genetic structure study of the non-native weed, common tansy (*Tanacetum vulgare*). *Canadian Journal of Plant Science*, *91*, 717–723.
Clements, D. R., & Ditommaso, A. (2011). Climate change and weed adaptation: Can evolution of invasive plants lead to greater range expansion than forecasted? *Weed Research*, *51*, 227–240.
Clements, D. R., & Jones, V. L. (2021). Rapid evolution of invasive weeds under climate change: Present evidence and future research needs. *Frontiers in Agronomy*, *3*, 664034. https://doi.org/10.3389/fagro.2021.664034
Cox, T. J., & Durrett, R. (2002). The stepping stone model: New formulas expose old myths. *The Annals of Applied Probability*, *12*, 1348–1377.
Cruzan, M. B., & Hendrickson, E. C. (2020). Landscape genetics of plants: Challenges and opportunities. *Plant Communications*, *1*, 100100.
DeMarche, M. L., Doak, D. F., & Morris, W. F. (2019). Incorporating local adaptation into forecasts of species' distribution and abundance under climate change. *Global Change Biology*, *25*, 775–793.
Di Cola, V., Broennimann, O., Petitpierre, B., Breiner, F. T., D'Amen, M., Randin, C., Engler, R., Pottier, J., Pio, D., Dubuis, A., Pellissier, L., Mateo, R. G., Hordijk, W., Salamin, N., & Guisan, A. (2017). ecospat: An R package to support spatial analyses and modeling of species niches and distributions. *Ecography*, *40*, 774–787.
Dlugosch, K. M., Anderson, S. R., Braasch, J., Cang, F. A., & Gillette, H. D. (2015). The devil is in the details: Genetic variation in introduced populations and its contributions to invasion. *Molecular Ecology*, *24*, 2095–2111.
Dlugosch, K. M., & Parker, I. M. (2008). Founding events in species invasions: Genetic variation, adaptive evolution, and the role of multiple introductions. *Molecular Ecology*, *17*, 431–449.
Dray, S., Dufour, A., & Chessel, D. (2007). The ade4 package-II: Two-table and K-table methods. *R News*, *7*, 47–52.
Dray, S., & Dufour, A.-B. (2007). The ade4 package: Implementing the duality diagram for ecologists. *Journal of Statistical Software*, *22*, 1–20.
Duforet-Frebourg, N., & Blum, M. G. B. (2014). Nonstationary patterns of isolation-by-distance: Inferring measures of local genetic differentiation with Bayesian kriging. *Evolution*, *68*, 1110–1123.
Dyer, R. J., Nason, J. D., & Garrick, R. C. (2010). Landscape modelling of gene flow: Improved power using conditional genetic distance derived from the topology of population networks. *Molecular Ecology*, *19*, 3746–3759.
EDDMapS. (2023). *Early Detection & Distribution Mapping System*. The University of Georgia - Center for Invasive Species and Ecosystem Health. http://www.eddmaps.org/
Etherington, T. R. (2015). Geographical isolation and invasion ecology. *Progress in Physical Geography: Earth and Environment*, *39*, 697–710.
Frankham, R. (2005). Resolving the genetic paradox in invasive species. *Heredity*, *94*, 385.
Gallien, L., Douzet, R., Pratte, S., Zimmermann, N. E., & Thuiller, W. (2012). Invasive species distribution models - how violating the equilibrium assumption can create new insights: Beyond the equilibrium assumption of SDMs. *Global Ecology and Biogeography*, *21*, 1126–1136.
Gorton, A. J., Tiffin, P., & Moeller, D. A. (2019). Does adaptation to historical climate shape plant responses to future rainfall patterns? A rainfall manipulation experiment with common ragweed. *Oecologia*, *190*, 941–953.
Goslee, S. C., & Urban, D. L. (2007). The ECODIST package for dissimilarity-based analysis of ecological data. *Journal of Statistical Software*, *22*, 1–19.
Guisan, A., Petitpierre, B., Broennimann, O., Daehler, C., & Kueffer, C. (2014). Unifying niche shift studies: Insights from biological invasions. *Trends in Ecology & Evolution*, *29*, 260–269.
Hallatschek, O., Hersen, P., Ramanathan, S., & Nelson, D. R. (2007). Genetic drift at expanding frontiers promotes gene segregation. *Proceedings of the National Academy of Sciences*, *104*, 19926–19930.
Hill, M. O., & Smith, A. J. E. (1976). Principal component analysis of taxonomic data with multi-state discrete characters. *Taxon*, *25*, 249–255.
Hodgins, K. A., Bock, D. G., & Rieseberg, L. H. (2018). Trait evolution in invasive species. *Annual Plant Reviews Online*, *1*, 1–37.
Hofmeister, N. R., Werner, S. J., & Lovette, I. J. (2021). Environmental correlates of genetic variation in the invasive European starling in North America. *Molecular Ecology*, *30*, 1251–1263.
Hutchison, D. W., & Templeton, A. R. (1999). Correlation of pairwise genetic and geographic measures: Inferring the relative influences of gene flow and drift on the distribution of genetic variability. *Evolution*, *53*, 1898–1914.
Ibrahim, K. M., Nichols, R. A., & Hewitt, G. M. (1996). Spatial patterns of genetic variation generated by different forms of dispersal during range expansion. *Heredity*, *77*, 282–291.
Jacobs, J. (2008). Ecology and management of common Tansy (*Tanacetum vulgare* L.). In *Invasive species technical note No. MT-18*. USDA Natural Resources Conservation Service.
Jombart, T. (2008). Adegenet: A R package for the multivariate analysis of genetic markers. *Bioinformatics*, *24*, 1403–1405.
Jombart, T., & Ahmed, I. (2011). adegenet 1.3-1: New tools for the analysis of genome-wide SNP data. *Bioinformatics*, *27*, 3070–3071.
Jombart, T., Devillard, S., Dufour, A.-B., & Pontier, D. (2008). Revealing cryptic spatial patterns in genetic variability by a new multivariate method. *Heredity*, *101*, 92–103.
Kawecki, T. J. (2008). Adaptation to marginal habitats. *Annual Review of Ecology, Evolution, and Systematics*, *39*, 321–342.
Keskitalo, M., Linden, A., & Valkonen, J. P. T. (1998). Genetic and morphological diversity of Finnish tansy. *Theoretical and Applied Genetics*, *9*, 6–1141.
Kimura, M. (1964). Diffusion models in population genetics. *Journal of Applied Probability*, *1*, 177–232.
Kimura, M., & Weiss, G. H. (1964). The stepping stone model of population structure and the decrease of genetic correlation with distance. *Genetics*, *49*, 561–576.
Klopfstein, S., Currat, M., & Excoffier, L. (2006). The fate of mutations surfing on the wave of a range expansion. *Molecular Biology and Evolution*, *23*, 482–490.
Lake, T. A., Briscoe Runquist, R. D., Flagel, L. E., & Moeller, D. A. (2023). Chronosequence of invasion reveals minimal losses of population genomic diversity, niche expansion, and trait divergence in the polyploid, leafy spurge. *Evolutionary Applications*, *16*, 1680–1696.
Lake, T. A., Briscoe Runquist, R. D., & Moeller, D. A. (2020). Predicting range expansion of invasive species: Pitfalls and best practices for obtaining biologically realistic projections. *Diversity and Distributions*, *26*, 1767–1779.
Lakoba, V. T., Atwater, D. Z., Thomas, V. E., Strahm, B. D., & Barney, J. N. (2021). A global invader's niche dynamics with intercontinental introduction, novel habitats, and climate change. *Global Ecology and Conservation*, *31*, e01848. https://doi.org/10.1016/j.gecco.2021.e01848
Leblois, R., Rousset, F., Tikel, D., Moritz, C., & Estoup, A. (2000). Absence of evidence for isolation by distance in an expanding cane toad (*Bufo marinus*) population: An individual-based analysis of microsatellite genotypes. *Molecular Ecology*, *9*, 1905–1909.
LeCain, R., & Sheley, R. (2014). Common tansy. In *Tanacetum vulgare*. Montana State University Extension: MontGuide MT199911AG.
Lee, C. E. (2002). Evolutionary genetics of invasive species. *Trends in Ecology and Evolution*, *17*, 386–391.

Legendre, P., Lapointe, F.-J., & Casgrain, P. (1994). Modeling brain evolution from behavior: A permutational regression approach. *Evolution*, *48*, 1487–1499.

Lu, S., Luo, X., Han, L., Yang, J., Jin, J., & Yang, J. (2022). Genetic patterns reveal differences between the invasion processes of common ragweed in urban and non-urban ecosystems. *Global Ecology and Conservation*, *38*, e02214.

Mack, R. N. (2003). Plant naturalizations and invasions in the eastern United States: 1634-1860. *Annals of the Missouri Botanical Garden*, *90*, 77–90.

Malinsky, M., Trucchi, E., Lawson, D. J., & Falush, D. (2018). RADpainter and fineRADstructure: Population inference from RADseq data. *Molecular Biology and Evolution*, *35*, 1284–1290.

Marcus, J., Ha, W., Barber, R. F., & Novembre, J. (2021). Fast and flexible estimation of effective migration surfaces. *eLife*, *10*, e61927.

Matula, D. W., & Sokal, R. R. (2010). Properties of Gabriel graphs relevant to geographic variation research and the clustering of points in the plane. *Geographical Analysis*, *12*, 205–222.

Mitich, L. W. (1992). Tansy. *Weed Technology*, *6*, 242–244.

MN Department o of Agriculture: Common Tansy. (2023). *Common Tansy*. Minnesota Department of Agriculture. https://www.mda.state.mn.us/plants/pestmanagement/weedcontrol/noxiouslist/commontansy

MN Department of Natural Resources Ecological Classification System. (2023). Ecological Classification System. https://www.dnr.state.mn.us/ecs/index.html

MN Department of Natural Resources: Common Tansy. (2023). *Common Tansy*. Minnesota Department of Natural Resources. https://www.dnr.state.mn.us/invasives/terrestrialplants/herbaceous/commontansy.html

Mouquet, N., Lagadeuc, Y., Devictor, V., Doyen, L., Duputié, A., Eveillard, D., Faure, D., Garnier, E., Gimenez, O., Huneman, P., Jabot, F., Jarne, P., Joly, D., Julliard, R., Kéfi, S., Kergoat, G. J., Lavorel, S., le Gall, L., Meslin, L., … Loreau, M. (2015). Predictive ecology in a changing world. *The Journal of Applied Ecology*, *52*, 1293–1310.

Moyle, L. C. (2006). Correlates of genetic differentiation and isolation by distance in 17 congeneric silene species. *Molecular Ecology*, *15*, 1067–1081.

Nei, M., Maruyama, T., & Chakraborty, R. (1975). The bottleneck effect and genetic variability in populations. *Evolution*, *29*, 1–10.

Novembre, J., & Stephens, M. (2008). Interpreting principal component analyses of spatial population genetic variation. *Nature Genetics*, *40*, 646–649.

Nychka, D., Furrer, R., Paige, J., & Sain, S. (2021). *Fields: Tools for spatial data*. University Corporation for Atmospheric Research.

Oduor, A. M. O., Leimu, R., & van Kleunen, M. (2016). Invasive plant species are locally adapted just as frequently and at least as strongly as native plant species. *The Journal of Ecology*, *104*, 957–968.

Peter, B. M., & Slatkin, M. (2013). Detecting range expansions from genetic data. *Evolution*, *67*, 3274–3289.

Peterman, W. E. (2018). ResistanceGA: An R package for the optimization of resistance surfaces using genetic algorithms. *Methods in Ecology and Evolution*, *9*, 1638–1647.

Peterman, W. E., & Pope, N. S. (2021). The use and misuse of regression models in landscape genetic analyses. *Molecular Ecology*, *30*, 37–47.

Peterson, A. T., & Vieglais, D. A. (2001). Predicting species invasions using ecological niche modeling: New approaches from bioinformatics attack a pressing problem. *Bioscience*, *51*, 363–371.

Petitpierre, B., Broennimann, O., Kueffer, C., Daehler, C., & Guisan, A. (2017). Selecting predictors to maximize the transferability of species distribution models: Lessons from cross-continental plant invasions. *Global Ecology and Biogeography*, *26*, 275–287.

Petkova, D., Novembre, J., & Stephens, M. (2016). Visualizing spatial population structure with estimated effective migration surfaces. *Nature Genetics*, *48*, 94–100.

Prasad, A., Pedlar, J., Peters, M., McKenney, D., Iverson, L., Matthews, S., & Adams, B. (2020). Combining US and Canadian forest inventories to assess habitat suitability and migration potential of 25 tree species under climate change. *Diversity and Distributions*, *26*, 1142–1159.

Pritchard, J. K., Stephens, M., & Donnelly, P. (2000). Inference of population structure using multilocus genotype data. *Genetics*, *155*, 945–959.

Purcell, S. (2019). PLINK v. 1.9. http://pngu.mgh.harvard.edu/purcell/plink/

Purcell, S., Neale, B., Todd-Brown, K., Thomas, L., Ferreira, M. A. R., Bender, D., Maller, J., Sklar, P., de Bakker, P. I. W., Daly, M. J., & Sham, P. C. (2007). PLINK: A tool set for whole-genome association and population-based linkage analyses. *American Journal of Human Genetics*, *81*, 559–575.

Putra, A. R., Hodgins, K. A., & Fournier-Level, A. (2023). Assessing the invasive potential of different source populations of ragweed (*Ambrosia artemisiifolia* L.) through genomically informed species distribution modelling. *Evolutionary Applications*, *17*, e13632. https://doi.org/10.1111/eva.13632

R Core Team. (2021). *R: A language and environment for statistical computing*. R Foundation for Statistical Computing.

Räsänen, K., & Hendry, A. P. (2008). Disentangling interactions between adaptive divergence and gene flow when ecology drives diversification. *Ecology Letters*, *11*, 624–636.

Ray, A., & Ray, R. (2014). Rapid divergence of ecotypes of an invasive plant. *AoB Plants*, *6*, plu052.

Reich, D., Price, A. L., & Patterson, N. (2008). Principal component analysis of genetic data. *Nature Genetics*, *40*, 491–492.

Roberts, T. (1878). *Tanacetum vulgare. Bell Atlas detailed collection record information*. University of Minnesota Bell Museum Herbarium. https://bellatlas.umn.edu/collections/individual/index.php?occid=158375

Rochette, N. C., Rivera-Colón, A. G., & Catchen, J. M. (2019). Stacks 2: Analytical methods for paired-end sequencing improve RADseq-based population genomics. *Molecular Ecology*, *28*, 4737–4754.

Roman, J., & Darling, J. A. (2007). Paradox lost: Genetic diversity and the success of aquatic invasions. *Trends in Ecology and Evolution*, *22*, 454–464.

Savary, P., Foltête, J.-C., Moal, H., Vuidel, G., & Garnier, S. (2020). graph4lg: A package for constructing and analysing graphs for landscape genetics in R. *Methods in Ecology and Evolution*, *12*, 538–547.

Schlaepfer, D. R., Edwards, P. J., Widmer, A., & Billeter, R. (2008). Phylogeography of native ploidy levels and invasive tetraploids of *Solidago gigantea*. *Molecular Ecology*, *17*, 5245–5256.

Sexton, J. P., Hangartner, S. B., & Hoffmann, A. A. (2014). Genetic isolation by environment or distance: Which pattern of gene flow is most common? *Evolution*, *68*, 1–15.

Shafer, A. B. A., & Wolf, J. B. W. (2013). Widespread evidence for incipient ecological speciation: A meta-analysis of isolation-by-ecology. *Ecology Letters*, *16*, 940–950.

Slatkin, M. (1987). Gene flow and the geographic structure of natural populations. *Science*, *236*, 787–792.

Slatkin, M. (1993). Isolation by distance in equilibrium and non-equilibrium populations. *Evolution*, *47*, 264–279.

Slatkin, M., & Excoffier, L. (2012). Serial founder effects during range expansion: A spatial analog of genetic drift. *Genetics*, *191*, 171–181.

Taylor, D. R., & Keller, S. R. (2007). Historical range expansion determines the phylogenetic diversity introduced during contemporary species invasion. *Evolution*, *61*, 334–345.

Theoharides, K. A., & Dukes, J. S. (2007). Plant invasion across space and time: Factors affecting nonindigenous species success during four stages of invasion. *New Phytologist*, *176*, 256–273.

Thioulouse, J., Dray, S., Dufour, A.-B., Siberchicot, A., Jombart, T., & Pavoine, S. (2018). *Multivariate analysis of ecological data with ade4*. Springer.

Tomiolo, S., & Ward, D. (2018). Species migrations and range shifts: A synthesis of causes and consequences. *Perspectives in Plant Ecology, Evolution and Systematics*, *33*, 62–77.

USDA Plants Database. (2023). *Tanacetum vulgare* L. https://plants.usda.gov/home/plantProfile?symbol=TAVU

van Strien, M. J., Holderegger, R., & Van Heck, H. J. (2015). Isolation-by-distance in landscapes: Considerations for landscape genetics. *Heredity*, *114*, 27–37.

Veloz, S. D., Williams, J. W., Blois, J. L., He, F., Otto-Bliesner, B., & Liu, Z. (2012). No-analog climates and shifting realized niches during the late quaternary: Implications for 21st-century predictions by species distribution models. *Global Change Biology*, *18*, 1698–1713.

Wang, I. J., & Bradburd, G. S. (2014). Isolation by environment. *Molecular Ecology*, *23*, 5649–5662.

Wang, I. J., Glor, R. E., & Losos, J. B. (2013). Quantifying the roles of ecology and geography in spatial genetic divergence. *Ecology Letters*, *16*, 175–182.

White, D. J. (1997). *Tanacetum vulgare L: weed potential, biology, response to herbivory, and prospects for classical biological control in Alberta*. [Ph.D. Thesis]. University of Alberta, Department of Entomology.

White, D. J. (2001). *Tanacetum vulgare* L., common tansy (Asteraceae). In P. G. Mason & J. T. Huber (Eds.), *Biological Control Programmes in Canada, 1981-2000* (pp. 425–426). CABI Publishing.

Wolf, V. C., Gassmann, A., Clasen, B. M., Smith, A. G., & Müller, C. (2012). Genetic and chemical variation of *Tanacetum vulgare* in plants of native and invasive origin. *Biological Control*, *61*, 240–245.

Wolkovich, E. M., Cook, B. I., Allen, J. M., Crimmins, T. M., Betancourt, J. L., Travers, S. E., Pau, S., Regetz, J., Davies, T. J., Kraft, N. J. B., Ault, T. R., Bolmgren, K., Mazer, S. J., McCabe, G. J., McGill, B. J., Parmesan, C., Salamin, N., Schwartz, M. D., & Cleland, E. E. (2012). Warming experiments underpredict plant phenological responses to climate change. *Nature*, *485*, 494–497.

Wright, S. (1943). Isolation by distance. *Genetics*, *28*, 114–138.

Yang, F., Liu, N., Crossley, M. S., Wang, P., Ma, Z., Guo, J., & Zhang, R. (2020). Cropland connectivity affects genetic divergence of Colorado potato beetle along an invasion front. *Evolutionary Applications*, *39*, 920.

Yates, K. L., Bouchet, P. J., Caley, M. J., Mengersen, K., Randin, C. F., Parnell, S., Fielding, A. H., Bamford, A. J., Ban, S., Barbosa, A. M., Dormann, C. F., Elith, J., Embling, C. B., Ervin, G. N., Fisher, R., Gould, S., Graf, R. F., Gregr, E. J., Halpin, P. N., … Sequeira, A. M. M. (2018). Outstanding challenges in the transferability of ecological models. *Trends in Ecology and Evolution*, *33*, 790–802.

SUPPORTING INFORMATION

Additional supporting information can be found online in the Supporting Information section at the end of this article.

How to cite this article: Briscoe Runquist, R., & Moeller, D. A. (2024). Isolation by environment and its consequences for range shifts with global change: Landscape genomics of the invasive plant common tansy. *Molecular Ecology*, *33*, e17462. https://doi.org/10.1111/mec.17462